

Reengineering of the URT-0.5 Accelerator

M.E. Balezin, S.Yu. Sokovnin

*Institute of Electrophysics, Ural Branch RAS, 106 Amundsen St., 620216 Ekaterinburg, Russia;
Tel.: +7(3432) 678782, Fax: +7(3432) 67878794; sokovnin@iep.uran.ru*

Abstract – Tests of the URT-0.5 electron accelerator, which were performed to elucidate the outlooks for and the expediency of its use in radiation technologies, revealed some drawbacks of the accelerator design. The accelerator was reengineered to eliminate these drawbacks.

To improve the operating duty of the pulse transformer insulation, an additional inductance was installed in the circuit. Consequently, the transformer was protected from the pulsed overvoltage arising upon triggering of the semiconductor opening switch.

Thermal conditions of the outlet window foil of the vacuum diode were considerably improved thanks to the use of a metal ceramic cathode, which provided the distribution of the anode current free of local inhomogeneities. As a result, the lifetime of the outlet foil was extended.

A metal screen was placed around on the metal ceramic cathode to decrease the size of the electron beam.

The retrofit accelerator was installed in a processing line for sterilization of disposable medical items in individual packages.

1. Introduction

Electron accelerators, which are used in radiation technologies, should satisfy some requirements, such as effectiveness, stable parameters and reliability. The URT-0.5 electron accelerator [1] meets to a large extent these requirements. However, the practice of continuous operation of the accelerator revealed periodic breakdowns of the pulse transformer insulation. Moreover, when the accelerator was worked with a metal dielectric (MDM) cathode at pulse repetition rate approaching the limit (200 Hz), the foil in the outlet window of the vacuum diode overheated quickly. As a result, it failed and vacuum was broken, although the average (in time) density of the electron beam current ($8 \mu\text{A}/\text{cm}^2$) was nearly 30 times smaller than the limiting density ($0.26 \text{ mA}/\text{cm}^2$) [4]. This was due to local inhomogeneities in the current distribution over the foil where the current density was much larger than the average value.

The aforementioned drawbacks impeded the use of the accelerator in radiation technologies and necessitated its reengineering.

2. Description of Setup and Experimental Method

The URT-0.5 accelerator circuitry (Fig. 1) was amended so as to improve effectiveness and stability of the accelerator operation.

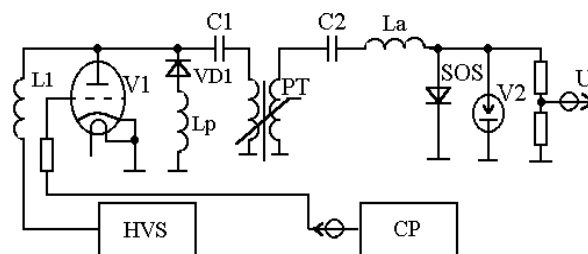


Fig. 1. HVS – high-voltage source; CU – control unit; L_1 , L_p , L_a – charging, recovery and additional inductances respectively; C_1 , C_2 – capacitances of the first and second circuits; PT – pulse transformer; VD1 – recovery diode; V1 – thyatron; V2 – vacuum diode; SOS – semiconductor opening switch

The thyatron circuit was supplemented with a recovery circuit comprising a diode type VD1 (SDL-800-0.4) and an inductance coil L_p . This circuit served to return residual energy, which was stored in the PT primary winding, to the storage capacitance C_1 upon its discharge. It is widely used in such circuitries [2]. The inductance L_p prohibited a pick of the current through the open diode, which could lead to the diode breakdown. The inductance value was selected experimentally. For this purpose, the voltage across the storage capacitance C_1 was measured using a capacitive voltage divider. It was found that the recovery circuit reduced the energy loss by 10%. The optimal value of the inductance coil was $L_p = 10.2 \mu\text{H}$.

To improve operating conditions of the PT insulation, the semiconductor opening switch (SOS) circuit was supplemented with an additional magnetic coil L_a , whose inductance ($L = 9.3 \mu\text{H}$) was optimized experimentally. The number of turns in the transformer secondary winding was cut twice in order to preserve the circuit inductance. By design, the magnetic coil comprised 5 turns of the RK-50 unbraided cable on a core 30 cm in diameter.

Standard electric transducers of the URT-0.5 accelerator, which were used in the experiments, provided measurements of the vacuum diode voltage and the beam current in the vacuum diode by means of a Tektronix TDS 360 digital oscilloscope.

3. Experimental Results and Conclusions

Results of the experiments concerned with the effect of the inductance L_a on parameters of the formed pulses are summarized in Table below.

Optimization of the circuit inductance ($L_a = 9.3 \mu\text{H}$) led to the increase in the amplitude of accelerating voltage pulses (Fig. 2). The length of voltage and current

Table. Experimental results

| L_a , μH | MDM cathode | | | MC cathode | | | Shielded MC cathode | | |
|-----------------------|-------------|-----------|------------|------------|-----------|------------|---------------------|-----------|------------|
| | U , kV | I_m , A | P_m , MW | U , kV | I_m , A | P_m , MW | U , kV | I_m , A | P_m , MW |
| 0 | 395 | 131 | 52 | 334 | 329 | 109 | 386 | 144 | 55 |
| 2.5 | 359 | 67 | 24 | 307 | 214 | 65 | 389 | 103 | 40 |
| 7.8 | 448 | 189 | 84 | 366 | 363 | 132 | 506 | 181 | 91 |
| 9.3 | 477 | 202 | 96 | 360 | 394 | 141 | 530 | 230 | 121 |
| 14.5 | 439 | 233 | 102 | 339 | 364 | 123 | 520 | 226 | 117 |

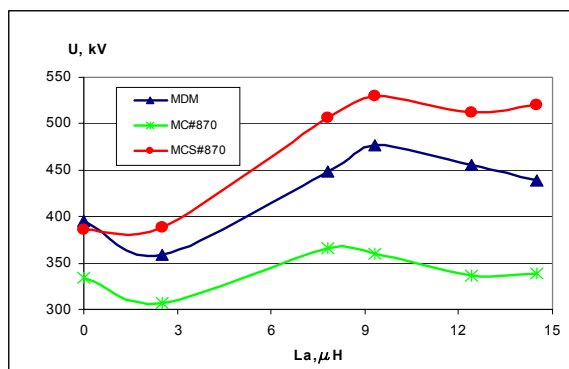


Fig. 2. Effect of the additional inductance on pulse voltage for MDM cathode, MC cathode and shielded MC

pulses decreased nearly by a factor of 1.5, while the time of a current pulse delay relative to a voltage pulse shortened (Fig. 3).

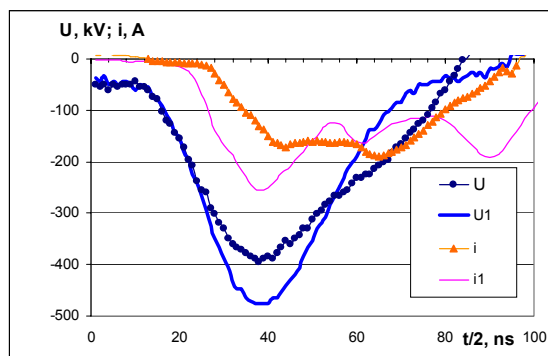


Fig. 3. Oscillograms of voltage and current pulses with (U_1, i_1) and without $L_a = 9.3 \mu\text{H}$ (U, i)

Measurements of the absorbed dose distribution in aluminum, which were made using CDP-2-F2 dosimeter films [3], are confirmed a considerable increase in penetrability of electrons (Fig. 4). Detectors were installed at a distance of 5 cm from the outlet window of the vacuum diode behind layers of an aluminum foil having different thickness. Measurements were made using 100 pulses applied at a frequency of 1 Hz.

To improve thermal conditions of the outlet foil, the standard MDM cathode was replaced by a metal-ceramic (MC) cathode, which provided a uniform distribution of the current over the anode [5]. As a result, the average density of the beam current density increased twice up to $17 \mu\text{A}/\text{cm}^2$. However, the MC

cathode decreased the vacuum diode impedance (Table and Fig. 2).

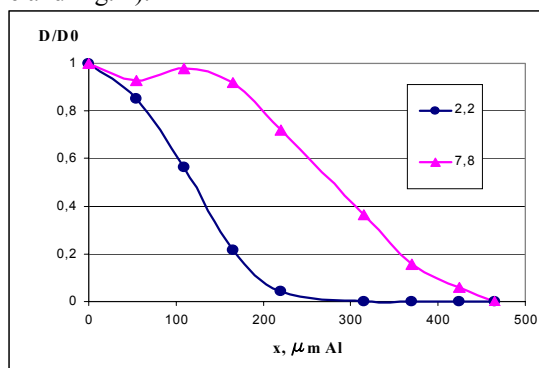


Fig. 4. Dose distributions in Al at different values of the inductance $L_a = 2.2$ and $7.8 \mu\text{H}$

The MC plate was the screened to decrease divergence of the electron beam in the MC cathode (Fig. 5).

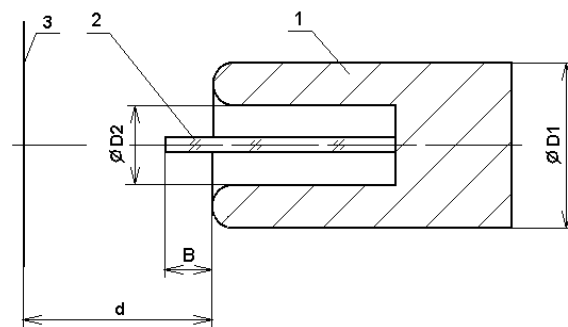


Fig. 5. Design of the shielded MC cathode: 1 – screen; 2 – MC plate; 3 – anode; D_2 and D_1 – inner and outer diameters of the screen

The effect of the MC cathode geometry on the vacuum diode characteristics was analyzed. The projection of the MC plate to the cathode-anode gap B (from -6 to 6 mm) and the screen diameter were variables in the experiments. Screens with the outer diameter of 30 and 40 mm and the inner diameter of 20 and 30 mm respectively were used.

It was found that when the cathode-to-anode distance was fixed at $d = 57$ mm and the MC plate was projected to the gap (the growth of B), the amplitude of accelerating voltage pulses dropped almost linearly, while the beam current increased (Fig. 6). The voltage decreased rather slowly, whereas the current value changed rapidly to a large extent, namely, several times. The dashed lines in Fig. 7 show for comparison voltage levels at the cathode without the MC plate (line 1) and without the screen (line 2).

When the MC plate was projected to the cathode-to-anode gap, the current increased sharply most probably because the screen had a weaker effect on the electric field distribution over the MC plate. The vacuum diode impedance dropped quickly as B increased from -6 mm to 0 and then remained constant.

The beam print on the detector with the screened MC cathode was shaped like an ellipse with the axis ratio

of 5:4. The large half-axis of the ellipse coincided with the plane of the MC plate. The beam was virtually homogeneous in the center, but the current density on the beam boundary was several times larger than the average density. Fig. 8 presents current distributions over the anode along the large axis ($d = 57$ mm) for different dimensions of the screening electrode and different projections B . Notice that the beam inhomogeneity observed for the screened MC cathode was not sharp and did not influence resistance of the outlet foil.

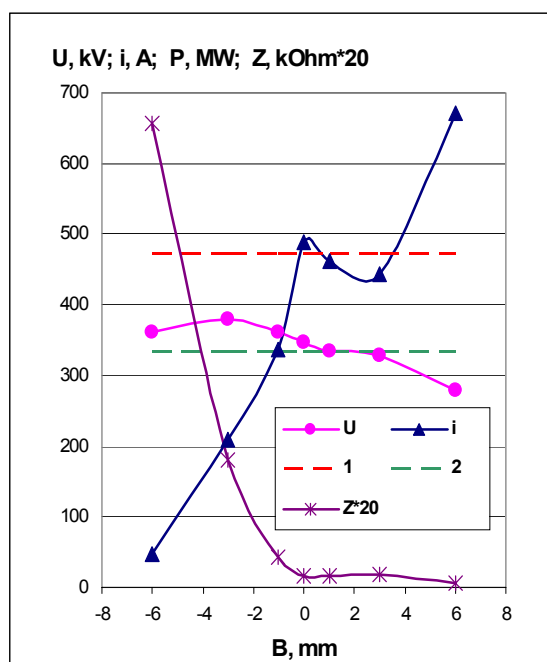


Fig. 6. Voltage (U), current (i) and impedance (Z) vs. projection (B) of the MC plate

It was found that the beam size increased with growing dimensions of the screen (at a fixed B) or projection of the plate to the gap (at a fixed dimension of the shield). It is very important for some applications that when the screen dimensions are fixed and B is constant, the beam size changes little with the cathode-to-anode distance d . The beam size changed more than twice with an MC cathode [5] without the screen.

On our opinion, reason of weak changing a beam size of screened MC cathode is concluded in change by screen an electrical field distribution along MC plates, with the result that emitted from plasma electrons are focused. This phenomenon is responsible for local inhomogeneity on edges of the beam too.

It should be noted that operation of the screened MC cathode was stable over the whole interval of B studied.

Thus, reengineering of the accelerator made it possible to

1) ensure a more stable operation of the accelerator and improve its effectiveness thanks to the use of an energy recovery circuit;

2) increase penetrability of accelerated electrons;
3) improve thermal conditions of the setup as a whole and prolong the lifetime of the foil in the outlet window of the vacuum diode in limiting operation regimes thanks to the use of an MC cathode;

4) control power and dimensions of the electron beam thanks to the installation of a screened MC cathode.

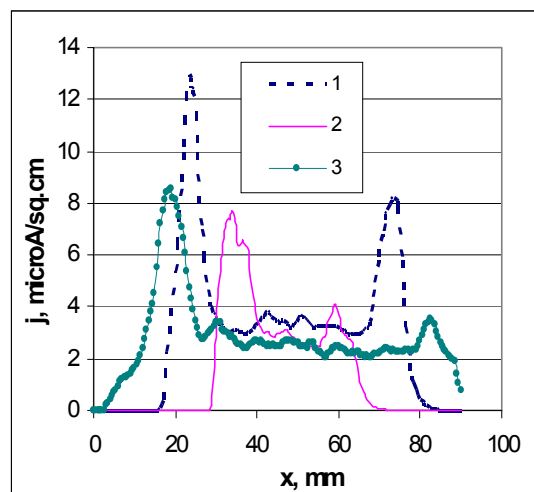


Fig. 7. Current distribution over the anode at different projections (B) of the MC plate and different dimensions of the screen (D_1/D_2): $B = -3$ and $40/30$ (1); $B = -3$ and $30/20$ (2); $B = 0$ and $30/20$ (3)

The modernized accelerator served as the basis of a line for sterilization of medical items in individual packages. Procedures of radiation sterilization of atraumatic needles with polyester or polypropylene surgical threads having conventional numbers from 1/0 to 6/0 and atraumatic needles with dissolving polyglycolide threads having conventional numbers 4/0, 3/0, 2/0 and 0 in polymer packages, which are produced by "Medin" Co. Ltd., have been approved by the RF Ministry of Health.

The authors thank Prof. Yu.A. Kotov for supervising this work, helpful comments and suggestions about earlier draft of this manuscript.

References

- [1] Yu.A. Kotov, S.Yu. Sokovnin, M.E. Balezin, PTE, No. 1, 112 (2000).
- [2] I.V. Grekhov, A.K. Kozlov, S.V. Korotkov, A.L. Stepanyants, PTE, No. 1, 70, (2000).
- [3] V.V. Generalova, M.N. Gursky, *Dosimetry in Radiation Technology*, Moscow, Iz-vo Standartov, 198 pp.
- [4] V.L. Auslender, I.L. Chertok, PTE, No. 6, 99 (1998).
- [5] Yu.A. Kotov, E.A. Litvinov, S.Yu. Sokovnin et al., DAN **370**, No. 3, 332 (2000).